# A building-scale hydrodynamic model for extreme urban flash flooding simulation: A Confluence Area in Raritan River Basin during Hurricane Ida

**Yifan Wang[1, *], Jie Gong[1], Chong Di[1]**

[1] *Rutgers, The State University of New Jersey, Department of Civil and Environmental Engineering, Piscataway, New Jersey, United States, 08854*
[*] *Correspondence: yw922@soe.rutgers.edu, +1-(551)-222-1091*

Abstract

**Under Climate change, especially Global Warming, the increased intensity and frequency of extreme precipitation events in more local areas have illustrated the importance of having a building-scaled flood forecasting system for urban risk management strategies. However, a building-scaled hydrodynamic model is rarely employed in operational forecasting, and the expositions of buildings' contribution to the flood dynamics in the urban environment are unsatisfactory. The present study aims to propose a framework for an operational flood forecasting system for the urban environment. We construct a parameter selection module to capture the time-varying nature of parameters in an operational hydrologic model. This framework was further applied with a focus on riverain flooding induced by Hurricane Ida. We find that the model would return similar or even better results by considering the time-varying nature of parameters. Besides, the prior hydro-conditions dominate the optimal parameter selection for a hydrologic model. The simulation results illustrate that excluding buildings from the computational mesh predicts shallower and slower flooding. We also find that adjusting manning's roughness would return comparable floodwater depth and duration but will cause significant bias in the simulated velocity and further impact the accuracy of advanced flood risk assessments.**

## 1. Introduction

As the climate changes, global warming enhances the potential of extreme weather, for example, bringing more precipitation falling to the northern areas and mountainous regions in the northeastern United States (Melillo et al.,

2014). The increase in intensity and frequency of rainfalls intensified local flooding (Kundzewicz et al., 2014), and better local flooding forecasting systems are needed to address this growing threat. There is a growing body of literature that recognizes the importance of having local-scaled flood forecasting models on local flood risk management strategies (Bessar et al., 2021; Ehret et al., 2008; Rehman et al., 2019; Xing et al., 2019)

Hydrologic Engineering Center's Hydrologic Modeling System (HEC-HMS) and River Analysis System (HEC-RAS) have been widely applied in inland flood-related research, such as compound flooding (F. Saleh et al., 2017), flash flooding (Alsubeai & Burckhard, 2021; Nguyen et al., 2015) and riverine flooding (Balbhadra et al., 2022; Ramachandran et al., 2019; Ynaotou et al., 2021). However, due to the computational cost, urban features like buildings are usually not included in the computational mesh. Thus, the expositions of buildings' contribution to the flood dynamics in the urban environment are unsatisfactory. Generally, Building's impacts on flooding dynamics, especially on flood depth, can be de-biased by model calibration, for example, adjusting manning's roughness (Garrote et al., 2021). However, the calibration will lead to over or underestimation of the flood velocity of the neighboring region of building features (Beretta et al., 2018). Flood velocity plays an important role in advanced flood damage and risk assessment in the built environment. For example, Specific Energy Height with a high correlation to building damage level requires both flood depth and velocity for calculation (Kreibich et al., 2009; Marvi, 2020; Schwarz & Maiwald, 2008). Moreover, findings from several studies suggest that flood velocity and duration contribute significantly to structural failure and building collapse during flooding (Gallegos et al., 2012; Jansen et al., 2020; Marvi, 2020; Sweet et al., 2017; Thieken et al., 2005). Besides, flood depth and flood velocity are dominant features in the human instability estimation during flooding (Milanesi et al., 2014; Wang & Marsooli, 2021b; Xia et al., 2014). All these studies about flood vulnerability for buildings and human bodies have spurred the need to predict better not only flood depth but also flood velocity for flood damage estimation and risk mitigation. Thus, with the growing computational power at the hands of hydrologists, it is necessary to include as many flood-related urban features as possible into urban hydrodynamic models.

Operational flood forecasting systems in the built environment are increasingly used by different agencies for emergency response during urban flooding. Extensive research has tried to couple HEC-HMS and HEC-RAS in flood conditions forecasting and hindcasting (Abdessamed & Abderrazak, 2019; Alsubeai & Burckhard, 2021; F. Saleh et al., 2017; Thakur et al., 2017). The reliability of the hindcasting simulation obtained using observed meteorological conditions depends on obtaining optimal parameter sets by calibration, a process to force the simulated flows to match historical observations. In a forecasting context, the accuracy of HEC-HMS hinges on the reliability of the meteorological inputs and the optimal set of model parameters during the forecast initiation phase. However, the optimal set of model parameters is time-varied because of the variation in soil moisture conditions. This time-varying nature in model parameters

should be captured in a framework designed for operational flood forecasting.

The first objective of this paper is to design and construct an integrated model framework for operational flood forecasting for the built environment. The second objective is to evaluate the urban features' contribution to the simulated flood characteristics in the built environment through a case study in Manville Township of New Jersey in the United States. More specifically, we first constructed an integrated model framework including buildings in the model grids. A 2-dimensional building scale hydrodynamic model coupled with HEC-RAS and HEC-HMS forms the core of this framework. Both HEC-HMS and HEC-RAS models are calibrated and validated with historical events. We then developed a new dynamic calibration approach, called parameter selection module for HEC-HMS, that the parameters would be defined based on the prior and subsequence hydro-conditions of the simulation time instead of assuming constant optimal parameters after calibration. This calibration approach would capture the time-varying nature of the hydrologic model parameters and contribute to decreasing the uncertainty caused by the varying soil moisture in an operational forecasting system. Finally, the flood conditions of Hurricane Ida in 2021 in the study area are reconstructed and compared based on computational grids including and excluding building features.

## 2. Materials and Methods

### 2.1 Study Areas and Hurricane Ida

Hurricane Ida landed in Louisiana on August 29$^{\text{th}}$, 2021, as an "extremely dangerous" category 4 storm with sustained winds of 150 mph. While it weakened into a tropical storm after it landed, Ida still brought torrential rains to the great New York metropolitan area at the night on September 1$^{\text{st}}$, 2021, causing numerous flash flood warnings and other water emergencies.

This study focuses on the Manville Township, located on the confluence of the Raritan River main stem and its tributary Millstone River (Figure 1). Manville has historically been prone to flood hazards induced by heavy precipitation during extreme weather events such as tropical cyclones. During Hurricane Ida in 2021, Manville Township was one of the areas that were severely affected by riverine flooding. The water depth in the nearby Raritan River reached a record of 8.43 meters, shattering the previous record of 8.26 meters during the Hurricane Floyd in 1999. The widespread flash flooding caused significant delays in search and rescue operations because many roads were impassable during the height of the storm. In Manville, 40% of the population are Minors under the age of 18 and seniors over the age of 65 (Bureau United States Census, 2021), and they are particularly vulnerable to flood events. An obvious way of reducing such vulnerability is to have reliable and accurate flood damage predictions and assessments, from which effective rebuilding strategies can be identified.

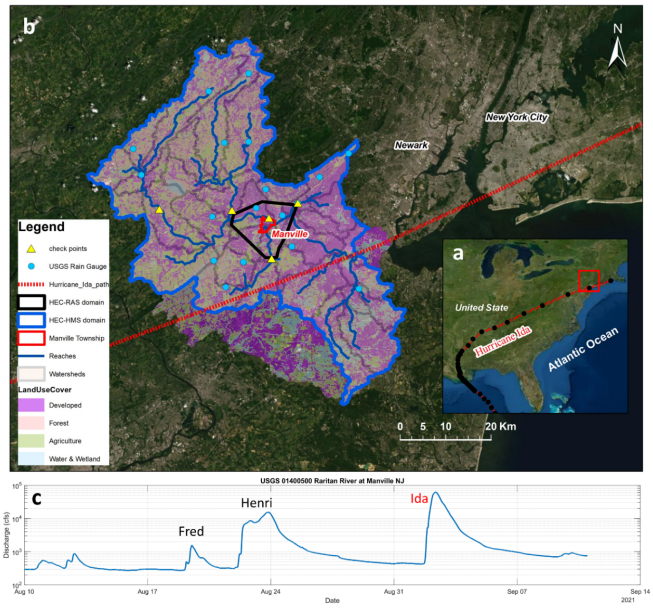


***Figure 1.*** (a) Manville Township, New Jersey, United States (red square) and the track of Hurricane Ida (red dash line) attacking New Jersey in the evening on September 1st. (b) The domain of the HEC-RAS model (black domain), the HEC-HMS (blue domain) model and its sub-basins (gray polygons), the Manville township municipal boundary (red domain), the locations of 17 rain gauges (blue dots), 5 USGS discharge gages (yellow triangles), and 4-type Land Use Covered layer used in the integrated model. (c) The observed river discharge was measured at Raritan River near the Manville Township before and after hurricane Ida.

### 2.2 Integrated model framework

The constructed flood model framework integrates a calibrated regional hydrologic modeling (HEC-HMS) and a calibrated 2-D hydrodynamic model (HEC-RAS) (Figure 2).

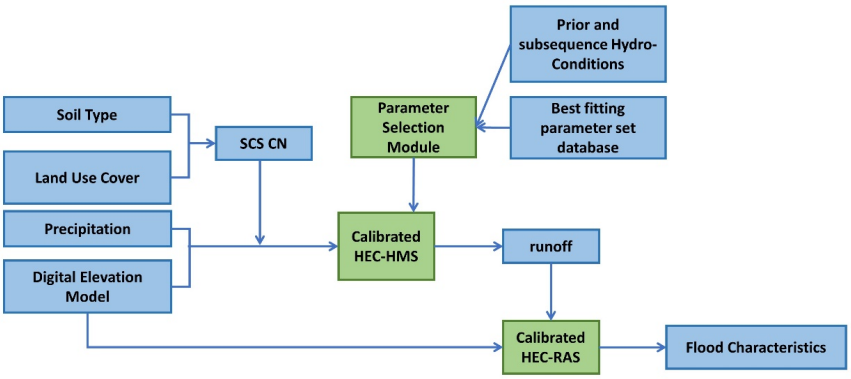


***Figure 2.*** Model framework

The Hydrologic Engineering Center's Hydrologic Modeling System (HEC-HMS) is a widely used conceptual semi-distributed hydrological model in rainfall-runoff related hydrological studies (City of New York, 2013; Hamdan et al., 2021; Ramaswamy & Saleh, 2020; Romali et al., 2018; F. Saleh et al., 2017; Zhang et al., 2013). It is designed to simulate the watershed runoff process by defining each basin using a series of empirically derived parameters that control the relationship between the system input and output (USACE, 2000).

The flood conditions including flood propagation and inundation level are simulated using the latest HEC-RAS 6 Hydrodynamic model. It solves the original shallow water equations (2-D Saint Venant Equations) using implicit finite volume algorithms (Brunner, 2021). HEC-RAS uses the sub-grid bathymetry method, achieved by calculating the relationship of the water depth vs. volume of each computational cell in the preprocessing. It keeps the details of the topography in the relatively coarse computational grid and allows a better representation of flow simulation (Brunner, 2021; F. Saleh et al., 2017). HEC-RAS has wide applications in flood-related studies, including but not limited to compound flooding (Loveland et al., 2021; F. Saleh et al., 2017), inland flash flooding (Abdessamed & Abderrazak, 2019; Buta et al., 2017; Costabile et al., 2020; Tamiru & Dinka, 2021), dam breach flooding (Bharath et al., 2021; Psomiadis et al., 2021), and sediment transportation (Shabani et al., 2021). In this study, a purely 2-D flow domain of HEC-RAS is selected using hydrologic conditions simulated by HEC-HMS boundary conditions.

In this integrated model framework, we creatively added a parameter selection module that is capable of automatically setting the optimal HEC-HMS parameter event by event to ensure the parameters represent the soil moisture

conditions as accurately as possible. Details about the module construction and application will be introduced in the following sections.

*2.2.1 HEC-HMS model setup*

The HEC-HMS domain covers 80% (152.94 $km^2$) of the Raritan River Basin area (Figure 1), and it was delineated into 38 sub-basins based on the flow direction and accumulation estimated from a digital elevation model (DEM). Each sub-basin is parameterized by a series of empirically derived parameters. In this study, the meteorological forcing for HEC-HMS such as precipitations is obtained from 15 United States Geological Survey (USGS) rain gages. They are assigned to the corresponding basins based on their distances to the basins. The Clark Unit Hydrograph method is used in the transform component to account for the characteristics of each basin over the study area. The recession method is used in the baseflow component to account for the groundwater contributions to the stream flow. The constructed HEC-HMS estimates the infiltration capacity and precipitation excess of each basin based on the Soil Conservation Service (SCS) curve number (CN) method. The default SCS CN value of each sub-basin is calculated based on the soil group raster dataset (ROSS et al., 2018), and the land use cover shapefile dataset (NJDEP, 2015) in ArcGIS (USACE, 2000). Both the Muskingum equations and the Lag equations are applied in the river routing components. Since the soil moisture variation could make differences in the estimated runoff by HEC-HMS (Firas Saleh et al., 2016), some critical parameters, such as initial abstraction, curve number, and impervious, are calibrated based on the observed flow data obtained from USGS gauges, to find the optimal combination of parameters.

*2.2.2 HEC-RAS model setup*

The HEC-RAS 2-D model domain covers part of the Raritan River Basin from the confluence of North Branch and South Branch in Branchburg to the Raritan River near Bound Brook Township, bounded by three major freshwater inputs, including the west bound of Raritan River, Royce Brook, Millstone River and Green Brook (Figure 1).

The creation of the model computational mesh and the model implementation requires detailed terrain information of the study area. The terrain information used in this study is mainly based on the combination of two DEMs and one reconstructed raster dataset. The first DEM is CoNED Topo-bathymetric Model for New Jersey and Delaware, 1880 to 2014 (OCM Partners, 2021), with a 1 meter spatial resolution and vertical accuracy ranging from 0.15 to 0.2 meter in root mean square error (RMSE). To improve the representation of bathymetry information in the first DEM dataset in the Raritan River main channel, sounding survey-based bathymetry information is necessary to be considered. Thus, the second DEM is the most recent Raritan River bathymetry dataset created by Rutgers University (Hunter, 2019) based on sounding surveys and NOAA navigational chart, with a 10-meter spatial resolution. A raster dataset of building footprints with a 1-meter spatial resolution was created based on the building

footprint data from Microsoft (Microsoft, 2021). The raster data is then merged onto the unified DEM to include the building features into the background geometry information.

The computational mesh for the HEC-RAS 2-D flow area contains 0.46 million cells in total, with spatially varied resolutions. In the study area, to resolve the building features, the mesh resolution is set to 10m x 10m. A coarser resolution (50m x 50m) in the rest of the domain area is used to save the computational expense.

The manning's roughness coefficient (N) and percent of impervious are estimated based on the land use cover dataset (NJDEP, 2015). They are treated as calibration parameters following the suggested range of values for each land cover type (U.S. Army Corps of Engineers, 2021) as shown in Table 3.

With an objective to evaluate the building features' influences on flood simulation results, the HEC-RAS model grid is set to include and exclude buildings in the background geometry information, respectively (Table 1). It has been suggested that in the case of excluding buildings, forcing the manning's roughness to 10 where buildings are located would return the closest flood conditions as that of the case of including buildings (Beretta et al., 2018). In this study, in the case of excluding buildings, we thereby forced the manning's roughness where buildings are located equal to 10.

@ >p(- 4) * >p(- 4) * >p(- 4) * @ & **HEC-RAS (Buildings Included)** & **HEC-RAS (Building Excluded)**
**DEM** &

Unified DEM based on:

1. *CoNED Topo-bathymetric Model for New Jersey and Delaware, 1880 to 2014*
2. *Raritan River bathymetry datasets from Rutgers University*
3. *Raster dataset of the building footprint from Microsoft*

&

Unified DEM based on:

1. *CoNED Topo-bathymetric Model for New Jersey and Delaware, 1880 to 2014*
2. *Raritan River bathymetry datasets from Rutgers University*

**Manning's Roughness** &

1. *Calibrated based on the land cover type*

&

1. *Forced to 10 at buildings' location*

2. *Same as the case of building included in the rest area.*

**Model Mesh Resolution** &

1. *10 meters in the town area*
2. *50 meters in the rest area of the domain*

& *Same as the case of building included*

***Table 1.***HEC-RAS model setup of the case of building included and of building excluded

*2.2.3 Calibration*

The constructed flood model is expected to apply to the study area for operational flash flooding forecasting in the future. Thus, in the HEC-HMS, we require a better representation of sub-basin characteristics that suit different events. Three parameters of loss models in HEC-HMS, including the initial abstraction ($I_a$), curve number (CN) and impervious (Imp) are calibrated based on hurricane Irene in 2011 and hurricane Henri in 2021, two major flood events in the study area. We carry out the calibration by both visual and statistical comparisons with the observed runoff obtained from 5 stations of USGS around the study area (Figure.1). The calibration is performed with a focus on the sub-basins where the stations are located. Considering the influence on downstream sub-basins from the upstream ones, the subsequence of calibrations depends on sub-basins' locations, from upstream to downstream. Calibration processes are implemented using a series of automated scripts that create a set of parameter combinations and execute the simulation. After the calibration process, a database of the best-fitting parameter sets is created and applied to the simulation of flooding in the area during Hurricane Ida. The details about the calibration are shown in Figure 3. To include all possible uncertainties caused by the calibrated parameters, we calculated the minimum required number of the parameters' combination based on the number of parameters and the polynomial degree of the loss model (Ghanem & Red-Horse, 2017; Nance, 2015) as the following function (Equation 1).

$$S = \frac{(n+p)!}{(n!p!)} \quad (1)$$

Where S is the minimum number of samples covering uncertainties, n is the number of parameters and p is the degree of the polynomial. Given the distributions of three calibrated parameters, the Latin hypercube sampling (LHS) method is employed to generate near-random samples. The distributions of all three calibrated parameters are assumed to be uniform (Table 2), with lower and upper bounds referring to the common range of these parameters of similar land use cover in literature (Brunner, 2021; Krajewski et al., 2020; Zheng et al., 2020). The actual correlation coefficient among three calibrated parameters in the generated near-random samples is limited no more than 0.015. Normalized

Nash–Sutcliffe model efficiency (NNSE) coefficient (Equation 2 - 3) is employed during the automatic calibration process to identify the best fitting parameter combination.

$$\text{NSE} = 1 - \frac{\sum_{t=1}^{T}(O_t - P_t)^2}{\sum_{t=1}^{T}(O_t - \overline{O})^2} \quad (2)$$

$$\text{NNSE} = \frac{1}{2 - NSE} \quad (3)$$

| Parameter | Distribution | Unit |
|---|---|---|
| **Initial Abstraction ($I_a$)** | *U (0,30)* | - |
| **Curve Number (CN)** | *U (60,95)* | - |
| **Impervious (Imp)** | *U (0,50)* | *%* |

***Table 2.*** Distribution of the loss model parameters of HEC-HMS. U stands for uniform distribution.

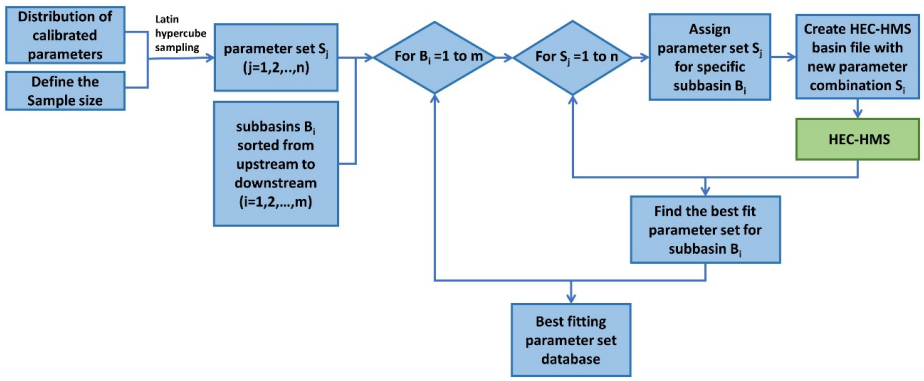


***Figure 3.*** framework of HEC-HMS calibration and the creation of best fitting parameter set database

The calibration in HEC-RAS focuses on manning's roughness coefficient, which is used to calculate the energy friction losses of overland flow and channel flow. It is usually determined based on the land use covers. In this study, the land use cover is obtained from the New Jersey Department of Environmental Protection (NJDEP). It defines the land use type using the modified Anderson classification system (MACS). Referring to the correspondence between Nation Land Cover Data (NLCD) and MACS, the range of manning's roughness of four land type classes 1) water, 2) developed, 3) barren land, and 4) forest are defined following the suggested values (U.S. Army Corps of Engineers, 2021), as shown

in Table 3. During calibration, the 10 combinations of manning's roughness of four land use types are created using LHS method. All manning's roughness of four classifications is uniform and random distributed among the generated 10 combinations. This study calibrates the manning's roughness by comparing the output floodwater depth with measured high-water mark (HWM) obtained by USGS. In the study area, there are a total of 27 HWM observations available for Hurricane Ida. Due to the lack of measured HWM data during other events, only Hurricane Ida was considered in the calibration and validation process.

| **MACS** | **NLCD** | **Range** | **Range for Calibration** |
|---|---|---|---|
| **Water** | *11 Open Water* | *0.025 - 0.05* | ***0.025 - 0.05*** |
| | *12 Perennial Ice/Snow* | - | |
| **Developed** | *21 Low Intensity Residential* | *0.03 - 0.05* | ***0.03 - 0.16*** |
| | *22 High Intensity Residential* | *0.06 - 0.12* | |
| | *23 Commercial/Industrial/Transportation* | *0.08 - 0.16* | |
| **Barren** | *31 Bare Rock/Sand/Clay* | *0.023 - 0.03* | ***0.023 - 0.03*** |
| | *32 Quarries/Strip Mines/Gravel Pits* | - | |
| | *33 Transitional* | - | |
| **Forested Upland** | *41 Deciduous Forest* | *0.1 - 0.2* | ***0.08 - 0.2*** |
| | *42 Evergreen Forest* | *0.08 - 0.16* | |
| | *43 Mixed Forest* | *0.08 - 0.2* | |

***Table 3.*** The range of Manning's roughness during HEC-RAS calibration

## 3. Results

### 3.1 HEC-HMS model calibration

After figuring out the best fitting parameter combination for each calibrated sub-basin as a sequence from upstream to downstream, we find the best fitting combinations for two calibration events are different. Since the three calibrated parameters are sensitive to soil moisture, the parameter combination used for the validation event or other major events will be selected based on the soil moisture conditions. Here we constructed a selection function of the previous hydro-conditions represented by runoff volume in 5 days prior to the beginning of the simulation ($\mathrm{RV}_{-5}$) and the future hydro-conditions represented by total precipitation volume in 3 days subsequent to the beginning of the simulation ($\mathrm{PV}_{+3}$):

$$\mathrm{Index}_i = W_1 \left| \frac{\mathrm{RV}_{-5,verif} - \mathrm{RV}_{-5,cali}}{\mathrm{RV}_{-5,verif}} \right| + W_2 \left| \frac{\mathrm{PV}_{+3,verif} - \mathrm{PV}_{+3,cali}}{\mathrm{PV}_{+3,verif}} \right| \quad (4)$$

Where i represents the specific calibration event. $\mathrm{RV}_{-5,verif}$ and $\mathrm{PV}_{+3,verif}$ are the runoff volume and the total precipitation volume over the sub-basin of the verification event Hurricane Ida. $\mathrm{RV}_{-5,cali}$ and $\mathrm{PV}_{+3,cali}$ are the runoff volume and total precipitation of each calibration event. $W_1$ and $W_2$ are the weight

factors, indicating the weights of prior hydro-conditions and subsequence hydro-conditions, respectively. The sum of the two weight factors is 1. The set of parameter combination returning the smallest index value will be selected in the simulation of the validation event. In the study area, Hurricane Ida has more similar prior hydro-conditions with that of Hurricane Henri but more similar subsequent hydro-conditions with that of Hurricane Irene. The values of two weight factors indicate which prior or subsequent hydro-conditions contribute more to the parameter selections. To identify the values of weight factors, we tested with increasing the weight of prior hydro-conditions from 0 to 1 with 0.1 intervals. Results show that the best fitting weight factors would be 0.7 and 0.3 for the prior and subsequence hydro-condition, respectively, giving the highest model efficiency coefficients in each sub-basin (Figure 4). The simulation for Hurricane Ida illustrates that using a dynamic optimal set of parameters, considering the prior and subsequent hydro-conditions, would return similar or event better results than using a fixed optimal set of parameters (Figure 4).

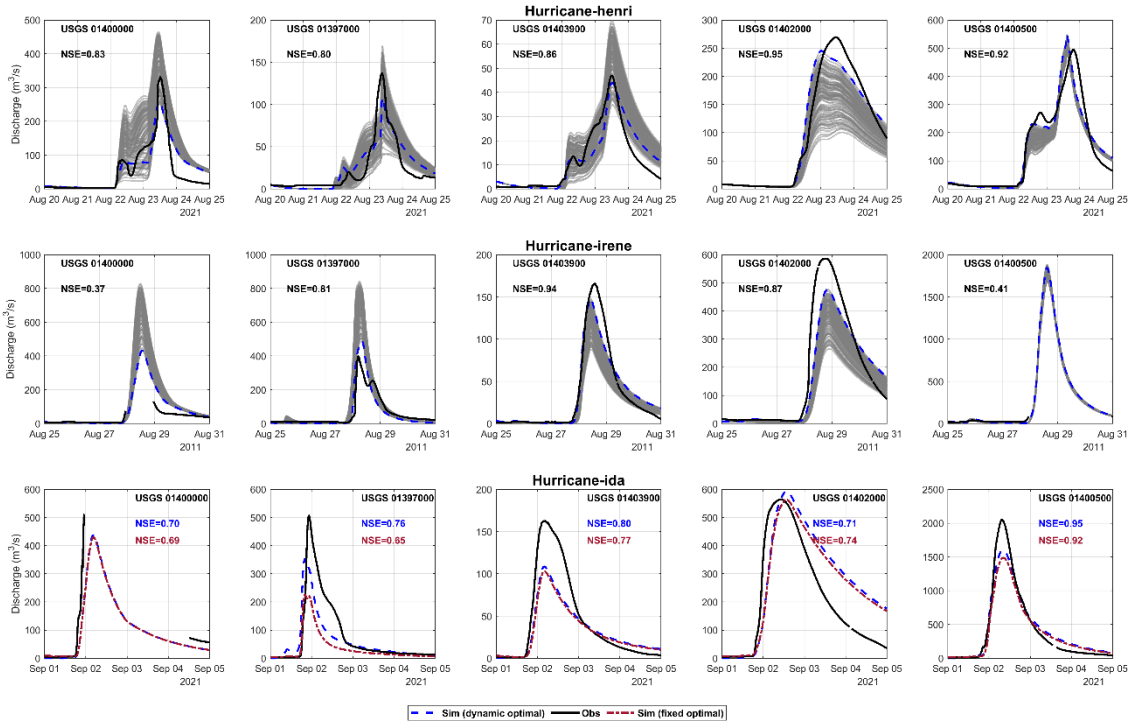


***Figure 4.*** The Calibration and Validation results at five check points. Gray lines represent the simulated runoff considering all uncertainty from the SCS curve number loss model. The black solid line is the observed discharge in $m^3/s$. The blue dash line is the simulation using the best fitting parameter combinations for the current event. The red dot-dash line in the sub-figures for the validation event, Ida, is the simulation using the fixed optimal parameter combinations.

### 3.2 Hurricane Ida

With the objective to simulate the flash flooding induced by Hurricane Ida in Manville Township, we forced the HEC-RAS model with the simulated runoff from the calibrated HEC-HMS model. The calibration and validation of HEC-RAS were constructed based on two statistic indexes, R-square (RSQ) and Absolute Mean Error (AME). Ten combinations of Manning's roughness for four classifications are created for calibration. Results show that the best fit of manning's roughness combinations in Manville Township is the one applied in test 10 with a relatively high RSQ of 0.858 and a relatively small AME of 0.12 meters (Figure 5).

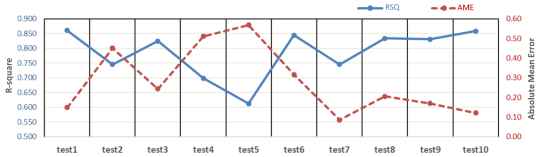


| | test1 | test2 | test3 | test4 | test5 | test6 | test7 | test8 | test9 | test10 | |
|---|---|---|---|---|---|---|---|---|---|---|---|
| Manning's | 0.048 | 0.032 | 0.032 | 0.029 | 0.026 | 0.046 | 0.039 | 0.041 | 0.046 | 0.037 | Water |
| Roughness in | 0.047 | 0.071 | 0.140 | 0.070 | 0.062 | 0.147 | 0.127 | 0.061 | 0.053 | 0.151 | Developed |
| Different | 0.023 | 0.025 | 0.028 | 0.028 | 0.025 | 0.026 | 0.024 | 0.029 | 0.030 | 0.027 | Barren |
| Test | 0.147 | 0.119 | 0.167 | 0.089 | 0.176 | 0.162 | 0.121 | 0.196 | 0.096 | 0.115 | Forested Upland |
| Comparison with HWM | | | | | | | | | | | |
| Statisitics | 0.86 | 0.75 | 0.82 | 0.70 | 0.61 | 0.84 | 0.75 | 0.83 | 0.83 | 0.86 | RSQ |
| | 0.15 | 0.45 | 0.24 | 0.51 | 0.57 | 0.32 | 0.09 | 0.21 | 0.17 | 0.12 | AME |

***Figure 5.*** The results of calibration and validation of the model. The top plot shows the R-square (blue solid line) and the Absolute Mean Error (red dash line) for all tests. The following tables show the corresponding manning's roughness of four land classifications in each test and the exact values of R-square and Absolute Mean Error for all tests.

Results illustrate that 43% (2.73 km2) of the area in Manville Township is flooded, impacting 24% of the buildings and 44% of the streets in the township (Figure 6. a). Among the inundated area, 10% of the area is located outside of the flood zone of FEMA, representing an area of 0.28 $km^2$ with a chance lower than 1% of prone to flooding were impacted by the flooding induced by hurricane Ida. Focusing on the flood conditions in the urban area, the maximum floodwater reaches more than 1.18 m in 50% of flooded areas and higher than 3.83 m in 5% of the flooded areas. Results indicate that the flood velocity remains relatively slow in the entire urban flooded area. The maximum flood speed is slower than 0.46 m/s in 95% of flooded areas, indicating that the flood water invaded the town slowly induced by the water level increase in the Raritan River due to the continued rainfall. More than 50% of the flooded area remained

as flooded for at least 18.83 hours.

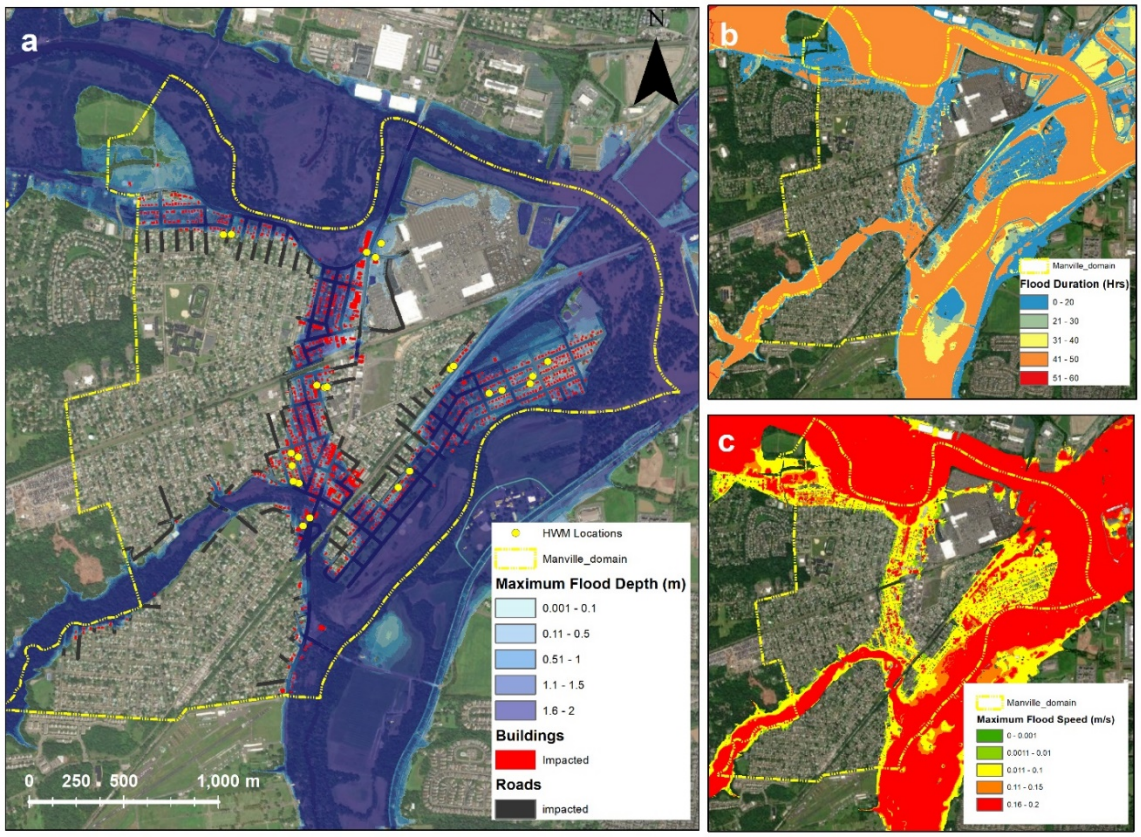


***Figure 6.*** An overview of the simulated flood conditions during hurricane Ida in Manville Township includes a) maximum flood depth in meters, b) flood duration in hours and c) maximum flood speed in meters per second. The location of the measured HWMs, impacted buildings and roads are also illustrated in a).

*3.2.1 The impacts of urban features*

We calculated and compared the scatter density among the maximum flood water depth, flood water velocity, and flood duration for both models including and excluding the building features in the computational mesh. The comparison results illustrate the urban feature impacts on flood characteristics in urban areas. To perform the comparison with a focus on urban areas, the permanent flood area (river channel and regulatory floodway) was excluded from the comparison. In general, the differences between the results of the two cases are relatively small, with the mean bias of -0.01-meter and -0.004 $m.s^{-1}$ for the flood water depth and velocity, respectively. The results show that excluding buildings from the computational mesh tends to predict more areas flooded by

shallower and slower flood water. It is illustrated that 99.4% and 75.4% of the urban flooded area show shallower maximum flood water depth and slower flood water velocity respectively in the case of excluding building features (Figure 7.d). In general, the underestimation of maximum water depth in the case of excluding building features is smaller than 5.2% in 90% of the urban flooded areas. In some local areas (5% urban flooded area), the maximum flood water depth and maximum flood water velocity are predicted at least 10.0% shallower and 55.1% slower in the case of excluding building features (Figure 7.d). In terms of flood duration, 47.3% of the urban flooded area shows shorter flooded duration when excluding building features. Similar to maximum flood water depth, the underestimation of flood duration is smaller than 5.1% in 90% of urban flooded areas (Figure 7.d). The heat difference maps shown in Figure 7, illustrate the difference between the scattering density of the two cases, excluding buildings and including buildings. A positive difference is represented in red color, indicating the case excluding buildings in the computational mesh predicts more area under specific flood conditions. The negative difference, represented in blue color, indicates the opposite. Results show that, compared with including buildings in the computational mesh, excluding buildings predicts at least 2 $km^2$ (31.5% area of Manville township) more areas experienced flood depth smaller than 1 meter and lasted for 5 to 15 hours (Figure 7.a). If we focus on the heat difference map of maximum flood velocity and maximum flood depth (Figure 7. b), it is obvious that a model excluding buildings predicts more area with maximum flood velocity slower than 0.2 m/s, where the maximum flood depth is shallower than 2 meters. It is also illustrated that the most increment of flood velocity heat maps occurs where flood duration varies from 5 to 20 hours (Figure 7. c).

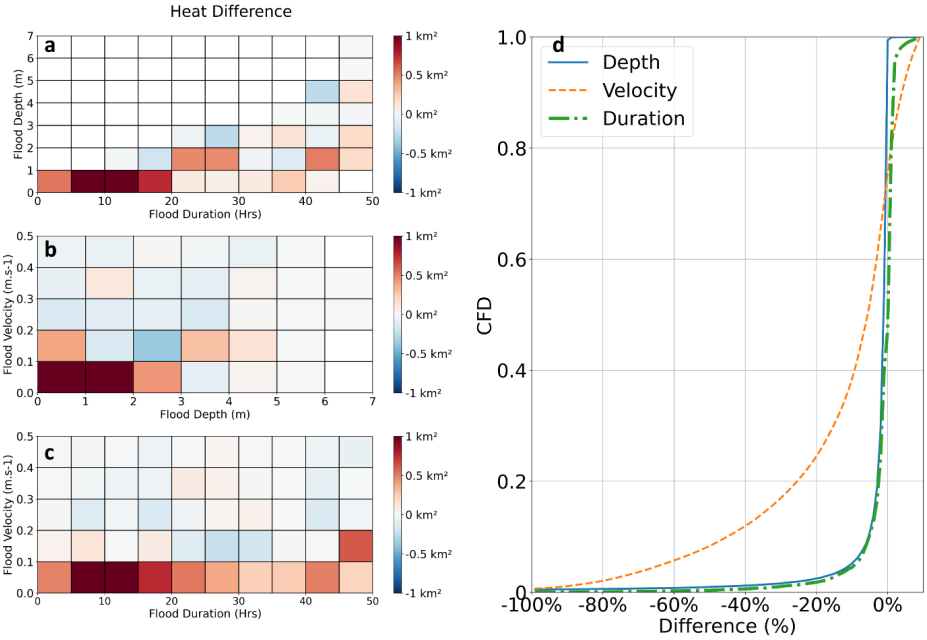


***Figure 7.*** The comparison between flood conditions in case of excluding and including building features in computational mesh, including the Heat Difference map of a) Flood Duration vs. Maximum Flood Depth, b) Maximum Flood Depth vs. Maximum Flood Velocity, and c) Flood Duration vs. Maximum Flood Velocity and d) the cumulative frequency distribution for the difference of maximum floodwater depth (blue solid line), velocity (orange dash line), and flood duration (green dash-dotted line). The heat difference maps are calculated by subtracting the scatter density of including buildings from those excluding buildings. Red color represents that the case excluding buildings in computational mesh simulates more area with specific flood conditions while blue represents the opposite.

## 4. Discussion

Prior studies have noted the superiority of using a hydrodynamic model compared with using the traditional bath-tubbing approach to predict flood hazards under the influence of building features in an urban area (Didier et al., 2019; Jordi et al., 2019; Marsooli & Wang, 2020; Wang & Marsooli, 2021a). This advantage is illustrated by considering the nonlinear interactions between floodwater depth and velocity and the flood extension variation induced by floodwater with different velocities in a built environment. Furthermore, a hydrodynamic model is capable of providing rich information for subsequent flood vulnerability assessments of buildings and individuals. As an integral part of flood risk management, hydrodynamic models have been widely applied in early warning systems at regional (Jordi et al., 2019; Ming et al., 2020), national (Werner

et al., 2009), continental (Emerton et al., 2016; Pappenberger et al., 2011) and global (Alfieri et al., 2013) scale. However, a building-scale hydrodynamic model is rarely employed in the system due to the expensive computational cost and the difficulties of conceptualizing the complicated urban environment. Under climate change, especially in northern areas and mountainous regions in the northeastern United States, more frequent and intensive precipitation will be expected, increasing the probability of one local area being prone to riverine and flash flooding. Compared to large-scale early warning systems, the residents and local emergency response department will be able to get ready more actively and effectively based on the flood forecasting at the meter-resolution. The framework developed in this study is part of an effort to develop an operational flood forecasting system, serving cities or townships under flood hazards.

Hydrodynamic models covering the built environments are usually constructed based on a bare-earth DEM, excluding building features, to increase numerical stability and save computational cost. This kind of simplification requires certain type of remedies, such as increasing the bottom friction where the buildings are located, to de-bias the dynamic impacts of building features on the flood depth. In this study, in case of excluding building features, the roughness coefficient was assumed as an extreme high value, simulating comparable floodwater depth and flood duration, with differences smaller than 5% in 90% of urban flooded area. After comparing the results of cases of excluding and including building features in the computational mesh, we found that the model excluding buildings predicts more area flooded by shallower and slower water. Since the Manville Township is in a low-lying and flat area, the flood water velocity during hurricane Ida is relatively slow, and the difference in the maximum flood water velocities is small. However, there is indeed a significant difference in maximum flood water velocity in cases of including and excluding building features in the computational mesh, at a 99% confidence level in the two-sample T-test. This finding illustrates that even though adjusting the manning roughness coefficient would return comparable floodwater depth and duration, it will cause significant bias in floodwater velocity and further impact the accuracy of advanced flood risk assessments. A hydrologic model with constant or fixed optimal parameters will cause uncertainties, especially in an operational flood forecasting system. The reason is that different events have different prior and subsequent hydro-conditions leading to different soil moisture conditions. It will further impact the tuning of the optimal parameters, such as curve numbers, initial abstractions, and impervious, of the hydrologic model. For example, those events that come with extremely heavy precipitation while the soil condition is initially dry would have totally different optimal parameters than those events with general precipitation while the soil condition is saturated. Also, in an operational system, with its continuous running, the prior and subsequent hydro-conditions keep changing with time, leading an issue that using a constant optimal parameter would not capture the time-varying nature of soil moisture condition. In this study, we developed a parameter selection module based on a selection function (Equation 4), to figure out the best fitting parameter set based on the

corresponding prior and subsequent hydro-conditions. In other words, the selection module will help the hydrologic model figure out the best fitting parameters case by case, to describe the correct soil moisture conditions. The weight factors $W_1$ and $W_2$ in the selection function illustrate that the prior hydro-conditions dominate the optimal parameter selection for a hydrologic model. The parameter selection module would be helpful in an operational flood forecasting system to decrease the uncertainty caused by using inappropriate parameters.

The relationship among prior and subsequent hydro-conditions and hydrologic model parameter selection is worthy of further study, in particular considering not only extreme events but also normal events. Abundant event samples would help an operational flooding forecasting system capture the time-varying nature of the hydrologic model parameters for different kinds of events. To apply this forecasting system operationally, forcing the model with ensembled predicted precipitation datasets from such as the Global Ensemble Forecast System (GEFS) and NOAA Quantitative Precipitation forecasts (QPF) should also be considered, to account for the uncertainties from the meteorological forcing datasets. These issues are critical to making the operational flood warning systems more robust and better support emergency response planning.

## 5. Summary and Conclusion

This study constructed a building-scaled hydrodynamic model to investigate the flood conditions during Hurricane Ida in Manville Township, New Jersey. The constructed flood model couples a calibrated 2-D hydrodynamic model (HEC-RAS) with a calibrated regional hydrologic modeling (HEC-HMS), and simulates the flood hazards, including flood water depth, velocity and duration, induced by Hurricane Ida.

The calibration of the regional hydrologic model (HEC-HMS) is implemented based on two historical events, hurricane Irene and Hurricane Henri. These two events have different prior and subsequent hydrologic conditions in the study area. For example, Hurricane Irene came with a large amount of direct precipitation while the soil was initial dry; Hurricane Henri came with a less amount of the subsequent direct precipitation while the soil was saturated due to a previous rainfall event. We found the best fit hydrologic parameters for these two extreme events are totally different, and it is hard to find a set of parameters to satisfy all extreme events. The finding reported here sheds new light on the hydrologic parameters' setup in hydrologic modeling, that the hydrologic parameters should be hydro-condition based or event-based. This study proposed a parameter selection module, to improve the hydrologic modeling by selecting the best fit parameter sets based on the hydro-conditions. It will decrease the uncertainty of a hydrologic model from using parameters inaccurate in representing the true soil moisture conditions. Another interesting finding out of developing the selection function is that the prior hydro-conditions usually dominate the selection of the parameters by gaining a larger weight factor in the function.

This study also shows that excluding building features from the computational mesh of hydrodynamic models could make a significant difference in the extreme flood water velocity. In the past studies, with an aim of saving computational cost, the computational mesh was usually created based on bare-earth DEMs, which exclude building features. The error caused by the simplification of topography is usually acceptable in regional or larger-scale hydrodynamic models. However, under climate change, with the increasing needs in high-resolution models, the dynamic impacts of building features on fluid need to be considered. One of the common methods used to de-bias the dynamic impacts of building features is to increase the bottom friction locally, especially where the building is located. This study compared two approaches to dealing with building features in a building-scaled hydrodynamic model, including or excluding building features (by increasing the bottom friction locally) in the computational mesh. The result has shown that excluding buildings from the computational mesh can simulate maximum floodwater depth and flood duration comparable to actual observations, but it tends to predict more areas flooded by shallower and slower peak floodwater. The result also pointed out that the decrease of the extreme floodwater velocity when building features are excluded is significant at the 99% confidence level when compared to simulations in which building features are included. In summary, this study provides a foundation to build a building-scaled operational flooding forecasting system, with an automatic hydraulics parameters selection module. The selection module takes into account the impacts of prior and subsequent hydro-conditions on runoff predictions. This decreases the uncertainties in an operational hydrologic model. When coupled with urban emergency responding systems or flood vulnerability models, the constructed flood forecasting system will contribute to flood preparedness at the local scale. The findings of this study also suggest that building-scaled flooding forecasting models should consider including building features into the computational mesh to take the dynamic impacts from buildings into account.

Acknowledgment
This research project was sponsored by U.S. National Science Foundation, under award #2103754 and FEMA 463198-A2020-80. The funding and support from U.S. National Science Foundation and FEMA are appreciated.

## Reference

Abdessamed, D., & Abderrazak, B. (2019). Coupling HEC-RAS and HEC-HMS in rainfall–runoff modeling and evaluating floodplain inundation maps in arid environments: case study of Ain Sefra city, Ksour Mountain. SW of Algeria. *Environmental Earth Sciences*, *78*(19), 586. https://doi.org/10.1007/s12665-019-8604-6Alfieri, L., Burek, P., Dutra, E., Krzeminski, B., Muraro, D., Thielen, J., & Pappenberger, F. (2013). GloFAS – global ensemble streamflow forecasting and flood early warning. *Hydrology and Earth System Sciences*, *17*(3), 1161–1175. https://doi.org/10.5194/hess-17-1161-2013Alsubeai, A., & Burckhard, S. R. (2021). Rainfall-Runoff Simulation and Modelling Using HEC-

HMS and HEC-RAS Models: Case Study Tabuk, Saudi Arabia. *Natural Resources*, *12*(10), 321–338. https://doi.org/10.4236/nr.2021.1210022Balbhadra, T., Ranjan, P., Ajay, K., Sajjad, A., & Ritu, G. (2022). Coupling HEC-RAS and HEC-HMS in Precipitation Runoff Modelling and Evaluating Flood Plain Inundation Map. In *World Environmental and Water Resources Congress 2017* (pp. 240–251). https://doi.org/doi:10.1061/9780784480625.022Beretta, R., Ravazzani, G., Maiorano, C., & Mancini, M. (2018). Simulating the influence of buildings on flood inundation in Urban areas. *Geosciences (Switzerland)*, *8*(2). https://doi.org/10.3390/geosciences8020077Bessar, M. A., Choné, G., Lavoie, A., Buffin-Bélanger, T., Biron, P. M., Matte, P., & Anctil, F. (2021). Comparative analysis of local and large-scale approaches to floodplain mapping: a case study of the Chaudière River. *Canadian Water Resources Journal / Revue Canadienne Des Ressources Hydriques*, *46*(4), 194–206. https://doi.org/10.1080/07011784.2021.1961610Bharath, A., Shivapur, A. V, Hiremath, C. G., & Maddamsetty, R. (2021). Dam break analysis using HEC-RAS and HEC-GeoRAS: A case study of Hidkal dam, Karnataka state, India. *Environmental Challenges*, *5*, 100401. https://doi.org/https://doi.org/10.1016/j.envc.2021.100401Brunner, G. W. (2021). *HEC-RAS HEC-RAS 2D User ' s Manual*. *January*, 171.Bureau United States Census. (2021). *QuickFacts: Manville borough, New Jersey*. United States Census Bureau.Buta, C., Mihai, G., & Stănescu, M. (2017). Flash floods simulation in a small drainage basin using HEC-RAS hydraulic model. *Ovidius University Annals of Constanta - Series Civil Engineering*, *19*(1), 101–118. https://doi.org/doi:10.1515/ouacsce-2017-0009City of New York. (2013). *a Stronger , More Resilient New York*. http://s-media.nyc.gov/agencies/sirr/SIRR_singles_Lo_res.pdfCostabile, P., Costanzo, C., Ferraro, D., Macchione, F., & Petaccia, G. (2020). Performances of the New HEC-RAS Version 5 for 2-D Hydrodynamic-Based Rainfall-Runoff Simulations at Basin Scale: Comparison with a State-of-the Art Model. In *Water* (Vol. 12, Issue 9). https://doi.org/10.3390/w12092326Didier, D., Baudry, J., Bernatchez, P., Dumont, D., Sadegh, M., Bismuth, E., Bandet, M., Dugas, S., & Sévigny, C. (2019). Multihazard simulation for coastal flood mapping: Bathtub versus numerical modelling in an open estuary, Eastern Canada. *Journal of Flood Risk Management*, *12*(S1), e12505. https://doi.org/https://doi.org/10.1111/jfr3.12505Ehret, U., Götzinger, J., Bárdossy, A., & Pegram, G. G. S. (2008). Radar-based flood forecasting in small catchments, exemplified by the Goldersbach catchment, Germany. *International Journal of River Basin Management*, *6*(4), 323–329. https://doi.org/10.1080/15715124.2008.9635359Emerton, R. E., Stephens, E. M., Pappenberger, F., Pagano, T. C., Weerts, A. H., Wood, A. W., Salamon, P., Brown, J. D., Hjerdt, N., Donnelly, C., Baugh, C. A., & Cloke, H. L. (2016). Continental and global scale flood forecasting systems. *WIREs Water* , *3*(3), 391–418. https://doi.org/https://doi.org/10.1002/wat2.1137Gallegos, H. A., Schubert, J. E., & Sanders, B. F. (2012). Structural Damage Prediction in a High-Velocity Urban Dam-Break Flood: Field-Scale Assessment of Predictive Skill. *Journal of Engineering Mechanics*, *138*(10),

1249–1262. https://doi.org/10.1061/(asce)em.1943-7889.0000427Garrote, J., González-Jiménez, M., Guardiola-Albert, C., & Díez-Herrero, A. (2021). The Manning's Roughness Coefficient Calibration Method to Improve Flood Hazard Analysis in the Absence of River Bathymetric Data: Application to the Urban Historical Zamora City Centre in Spain. In *Applied Sciences* (Vol. 11, Issue 19). https://doi.org/10.3390/app11199267Ghanem, R., & Red-Horse, J. (2017). Polynomial Chaos: Modeling, Estimation, and Approximation. In *Handbook of Uncertainty Quantification*. https://doi.org/10.1007/978-3-319-12385-1Hamdan, A. N., Almuktar, S., & Scholz, M. (2021). Rainfall-Runoff Modeling Using the HEC-HMS Model for the Al-Adhaim River Catchment, Northern Iraq. In *Hydrology* (Vol. 8, Issue 2). https://doi.org/10.3390/hydrology8020058Hunter, E. (2019). *Rartian River Basin Elevation Data*. Rutgers University.Jansen, L., Korswagen, P. A., Bricker, J. D., Pasterkamp, S., de Bruijn, K. M., & Jonkman, S. N. (2020). Experimental determination of pressure coefficients for flood loading of walls of Dutch terraced houses. *Engineering Structures*, *216*, 110647. https://doi.org/https://doi.org/10.1016/j.engstruct.2020.110647Jordi, A., Georgas, N., Blumberg, A., Yin, L., Chen, Z., Wang, Y., Schulte, J., Ramaswamy, V., Runnels, D., & Saleh, F. (2019). A Next-Generation Coastal Ocean Operational System: Probabilistic Flood Forecasting at Street Scale. *Bulletin of the American Meteorological Society*, *100*(1), 41–54. https://doi.org/10.1175/BAMS-D-17-0309.1Krajewski, A., Sikorska-Senoner, A. E., Hejduk, A., & Hejduk, L. (2020). Variability of the initial abstraction ratio in an urban and an agroforested catchment. *Water (Switzerland)*, *12*(2). https://doi.org/10.3390/w12020415Kreibich, H., Piroth, K., Seifert, I., Maiwald, H., Kunert, U., Schwarz, J., Merz, B., & Thieken, A. H. (2009). Is flow velocity a significant parameter in flood damage modelling? *Natural Hazards and Earth System Sciences*, *9*(5), 1679–1692. https://doi.org/10.5194/nhess-9-1679-2009Kundzewicz, Z. W., Kanae, S., Seneviratne, S. I., Handmer, J., Nicholls, N., Peduzzi, P., Mechler, R., Bouwer, L. M., Arnell, N., Mach, K., Muir-Wood, R., Brakenridge, G. R., Kron, W., Benito, G., Honda, Y., Takahashi, K., & Sherstyukov, B. (2014). Flood risk and climate change: global and regional perspectives. *Hydrological Sciences Journal*, *59*(1), 1–28. https://doi.org/10.1080/02626667.2013.857411Loveland, M., Kiaghadi, A., Dawson, C. N., Rifai, H. S., Misra, S., Mosser, H., & Parola, A. (2021). Developing a Modeling Framework to Simulate Compound Flooding: When Storm Surge Interacts With Riverine Flow . In *Frontiers in Climate* (Vol. 2).Marsooli, R., & Wang, Y. (2020). Quantifying Tidal Phase Effects on Coastal Flooding Induced by Hurricane Sandy in Manhattan, New York Using a Micro-Scale Hydrodynamic Model. *Frontiers in Built Environment*.Marvi, M. T. (2020). A review of flood damage analysis for a building structure and contents. *Natural Hazards*, *102*(3), 967–995. https://doi.org/10.1007/s11069-020-03941-wMelillo, J., Richmond, T. (T. C. ., & Yohe, G. (2014). *Climate Change Impacts in the United States: The Third National Climate Assessment*. https://doi.org/doi:10.7930/J0Z31WJ2Microsoft. (2021). *Building Footprints*. Microsoft.Milanesi, L., Pilotti, M., & Ranzi, R. (2014). A con-

ceptual model of people's vulnerability to floods. *Water Resource Research*, *51*, 2498–2514. https://doi.org/10.1002/2015WR017200.AMing, X., Liang, Q., Xia, X., Li, D., & Fowler, H. J. (2020). Real-Time Flood Forecasting Based on a High-Performance 2-D Hydrodynamic Model and Numerical Weather Predictions. *Water Resources Research*, *56*(7), e2019WR025583. https://doi.org/https://doi.org/10.1029/2019WR025583Nance, D. V. (2015). *Stochastic Estimation via Polynomial Chaos* (Issue October).Nguyen, H. Q., Degener, J., & Kappas, M. (2015). Flash Flood Prediction by Coupling KINEROS2 and HEC-RAS Models for Tropical Regions of Northern Vietnam. In *Hydrology* (Vol. 2, Issue 4). https://doi.org/10.3390/hydrology2040242NJDEP. (2015). *Land Use/Land Cover 2012 Update, Edition 20150217 Subbasin 02030105 - Raritan (Land_lu_2012_hu02030105)*.OCM Partners. (2021). *CoNED Topobathymetric Model for New Jersey and Delaware, 1880 to 2014*. NOAA National Centers for Environmental Information.Pappenberger, F., Thielen, J., & Del Medico, M. (2011). The impact of weather forecast improvements on large scale hydrology: Analysing a decade of forecasts of the European Flood Alert System. *Hydrological Processes*, *25*(7), 1091–1113. https://doi.org/10.1002/hyp.7772Psomiadis, E., Tomanis, L., Kavvadias, A., Soulis, K. X., Charizopoulos, N., & Michas, S. (2021). Potential Dam Breach Analysis and Flood Wave Risk Assessment Using HEC-RAS and Remote Sensing Data: A Multicriteria Approach. In *Water* (Vol. 13, Issue 3). https://doi.org/10.3390/w13030364Ramachandran, A., Palanivelu, K., Mudgal, B. V, Jeganathan, A., Guganesh, S., Abinaya, B., & Elangovan, A. (2019). Climate change impact on fluvial flooding in the Indian sub-basin: A case study on the Adyar sub-basin. *PLOS ONE*, *14*(5), e0216461.Ramaswamy, V., & Saleh, F. (2020). Ensemble Based Forecasting and Optimization Framework to Optimize Releases from Water Supply Reservoirs for Flood Control. *Water Resources Management*, *34*(3), 989–1004. https://doi.org/10.1007/s11269-019-02481-8Rehman, S., Sahana, M., Hong, H., Sajjad, H., & Ahmed, B. Bin. (2019). A systematic review on approaches and methods used for flood vulnerability assessment: framework for future research. *Natural Hazards*, *96*(2), 975–998. https://doi.org/10.1007/s11069-018-03567-zRomali, N. S., Yusop, Z., & Ismail, A. Z. (2018). Hydrological Modelling using HEC-HMS for Flood Risk Assessment of Segamat Town, Malaysia. *IOP Conference Series: Materials Science and Engineering*, *318*, 12029. https://doi.org/10.1088/1757-899x/318/1/012029ROSS, C. W., PRIHODKO, L., ANCHANG, J., KUMAR, S., JI, W., & HANAN, N. P. (2018). *Global Hydrologic Soil Groups (HYSOGs250m) for Curve Number-Based Runoff Modeling*. ORNL Distributed Active Archive Center. https://doi.org/10.3334/ORNLDAAC/1566Saleh, F., Ramaswamy, V., Wang, Y., Georgas, N., Blumberg, A., & Pullen, J. (2017). A multi-scale ensemble-based framework for forecasting compound coastal-riverine flooding: The Hackensack-Passaic watershed and Newark Bay. *Advances in Water Resources*, *110*. https://doi.org/10.1016/j.advwatres.2017.10.026Saleh, Firas, Ramaswamy, V., Georgas, N., Blumberg, A. F., & Pullen, J. (2016). A retrospective streamflow ensemble forecast for an extreme hydrologic event: A case study of Hurricane Irene and on the Hudson River basin. *Hydrology*

*and Earth System Sciences*, *20*(7), 2649–2667. https://doi.org/10.5194/hess-20-2649-2016Schwarz, J., & Maiwald, H. (2008). *DAMAGE AND LOSS PREDICTION MODEL BASED ON THE VULNERABILITY OF BUILDING TYPES*.Shabani, A., Woznicki, S. A., Mehaffey, M., Butcher, J., Wool, T. A., & Whung, P.-Y. (2021). A coupled hydrodynamic (HEC-RAS 2D) and water quality model (WASP) for simulating flood-induced soil, sediment, and contaminant transport. *Journal of Flood Risk Management*, *14*(4), e12747. https://doi.org/https://doi.org/10.1111/jfr3.12747Sweet, W. V, Horton, R., Kopp, R. E., LeGrande, A. N., & Romanou, A. (2017). Sea level rise. In D. J. Wuebbles, D. W. Fahey, K. A. Hibbard, D. J. Dokken, B. C. Stewart, & T. K. Maycock (Eds.), *Climate Science Special Report: Fourth National Climate Assessment, Volume I* (pp. 333–363). U.S. Global Change Research Program. https://doi.org/10.7930/J0VM49F2Tamiru, H., & Dinka, M. O. (2021). Application of ANN and HEC-RAS model for flood inundation mapping in lower Baro Akobo River Basin, Ethiopia. *Journal of Hydrology: Regional Studies*, *36*, 100855. https://doi.org/https://doi.org/10.1016/j.ejrh.2021.100855Thakur, B., Parajuli, R., Kalra, A., Ahmad, S., & Gupta, R. (2017). Coupling HEC-RAS and HEC-HMS in Precipitation Runoff Modelling and Evaluating Flood Plain Inundation Map. *World Environmental and Water Resources Congress 2017: Hydraulics and Waterways and Water Distribution Systems Analysis - Selected Papers from the World Environmental and Water Resources Congress 2017*, 240–251. https://doi.org/10.1061/9780784480625.022Thieken, A. H., Müller, M., Kreibich, H., & Merz, B. (2005). Flood damage and influencing factors: New insights from the August 2002 flood in Germany. *Water Resources Research*, *41*(12). https://doi.org/https://doi.org/10.1029/2005WR004177U.S. Army Corps of Engineers. (2021). Creating Land Cover, Manning's n Values, and Impervious Layers. *HEC-RAS 2D User's Manual*.USACE. (2000). Hydrologic Modeling System Technical Reference Manual. *HEC-HMS Technical Reference Manual*, *March*, 148.Wang, Y., & Marsooli, R. (2021a). Dynamic modeling of sea-level rise impact on coastal flood hazard and vulnerability in New York City's built environment. *Coastal Engineering*, *169*, 103980. https://doi.org/https://doi.org/10.1016/j.coastaleng.2021.103980Wang, Y., & Marsooli, R. (2021b). Physical Instability of Individuals Exposed to Storm-Induced Coastal Flooding: Vulnerability of New Yorkers During Hurricane Sandy. *Water Resources Research*, *57*(1), e2020WR028616. https://doi.org/https://doi.org/10.1029/2020WR028616Werner, M., Cranston, M., Harrison, T., Whitfield, D., & Schellekens, J. (2009). Recent developments in operational flood forecasting in England, Wales and Scotland. *Meteorological Applications*, *16*(1), 13–22. https://doi.org/https://doi.org/10.1002/met.124Xia, J., Falconer, R. A., Wang, Y., & Xiao, X. (2014). New criterion for the stability of a human body in floodwaters. *Journal of Hydraulic Research*, *52*(1), 93–104. https://doi.org/10.1080/00221686.2013.875073Xing, Y., Liang, Q., Wang, G., Ming, X., & Xia, X. (2019). City-scale hydrodynamic modelling of urban flash floods: the issues of scale and resolution. *Natural Hazards*, *96*(1), 473–496. https://doi.org/10.1007/s11069-018-3553-zYnaotou, Jayadi, R., Rahardjo, A. P., & Puspitosari, D. A. (2021). Identification of Flood-prone Areas using

HEC-HMS and HEC-RAS, the Case of Ciberang River Basin, Lebak District of Banten Province. *IOP Conference Series: Earth and Environmental Science*, *930*(1), 012082. https://doi.org/10.1088/1755-1315/930/1/012082Zhang, H. L., Wang, Y. J., Wang, Y. Q., Li, D. X., & Wang, X. K. (2013). The effect of watershed scale on HEC-HMS calibrated parameters: a case study in the Clear Creek watershed in Iowa, US. *Hydrology and Earth System Sciences*, *17*(7), 2735–2745. https://doi.org/10.5194/hess-17-2735-2013Zheng, Y., Li, J., Dong, L., Rong, Y., Kang, A., & Feng, P. (2020). Estimation of Initial Abstraction for Hydrological Modeling Based on Global Land Data Assimilation System–Simulated Datasets. *Journal of Hydrometeorology*, *21*(5), 1051–1072. https://doi.org/10.1175/JHM-D-19-0202.1